Noradrenergic input from nucleus of the solitary tract regulates parabrachial activity in mice

Chimdiya Onwukwe[1,3]*, Yadong Ji[2]*, Jesse Smith[1,3], Hanna Laub[1], Luca Posa[1], Asaf Keller[1,3,4], Radi Masri[1,2,3,4], Nathan Cramer[1,3,4]

*The first two authors contributed equally to this study.

[1]Department of Anatomy & Neurobiology, University of Maryland School of Medicine, Baltimore, Maryland 21201, and

[2]Department of Advanced Oral Sciences and Therapeutics, University of Maryland School of Dentistry, Baltimore, Maryland 21201, and

[3]Program in Neuroscience, University of Maryland School of Medicine, Baltimore, Maryland 21201, and

[4]Center to Advance Chronic Pain Research, University of Maryland School of Medicine, Baltimore, Maryland 21201

Corresponding authors: Nathan Cramer, ncramer@som.umaryland.edu

Radi Masri, rmasri@umaryland.edu

The authors declare that they have no competing financial interests.

Acknowledgements: Research reported in this publication was supported by the National Institute of Neurological Disorders and Stroke of the National Institutes of Health grants R01NS099245 and R01NS069568. The content is solely the responsibility of the authors and does not necessarily represent the official views of the National Institutes of Health. The funding sources had no role in study design; the collection, analysis and interpretation of data; the writing of the report; or in the decision to submit the article for publication.

Abstract

The parabrachial complex (PB) is critically involved in aversive processes, and chronic pain is associated with amplified activity of PB neurons in rodent models of neuropathic pain. Here we demonstrate that catecholaminergic input from the caudal nucleus of the solitary tract ($cNTS_{cat}$)—a stress responsive region that integrates intero- and exteroceptive signals—causes amplification of PB activity and their sensory afferents. Using a virally mediated expression of a norepinephrine (NE) sensor, NE2h, and fiber photometry in anesthetized mice, noxious mechanical and thermal stimuli caused prolonged NE transients in PB that far outlast the noxious stimulus. Similar NE transients in PB were evoked by focal stimulation of the superficial cNTS, a region that contains the noradrenergic A2 cell group that projects densely upon PB. *In vitro*, optical stimulation of $cNTS_{cat}$ terminals depolarized PB neurons and increased their frequency of spontaneous excitatory synaptic inputs. A dual opsin approach showed that sensory afferents from the caudal spinal trigeminal nucleus (SpVc) are potentiated by $cNTS_{cat}$ terminal activation. This potentiation was coupled with a decrease in the paired pulse ratio, consistent with an $cNTS_{cat}$ -mediated increase in the probability of release at SpVc synapses. Together, these data suggest that A2 neurons of the cNTS generate long lasting NE transients in PB which increase excitability and potentiate responses of PB neurons to sensory inputs. These reveal a mechanism through which stressors from multiple modalities may potentiate the aversiveness of nociceptive stimuli.

Keywords: Aversion; pain; nociception; interoceptive; exteroceptive; presynaptic potentiation.

Significance Statement

The aversiveness of pain is influenced by many factors, including physiological and emotional stress. We show that the parabrachial nucleus (PB), a key integrative hub for aversive stimuli, experiences prolonged norepinephrine transients following noxious stimulation in mice. These NE transients potentiate sensory input to PB and arise, at least in part, from catecholaminergic projections from the stress-responsive caudal nucleus of the solitary tract ($cNTS_{cat}$). We propose that activity this $cNTS_{cat}$ to PB pathway may potentiate the aversiveness of pain in stressful conditions.

Introduction

Chronic pain profoundly affects quality of life (Dworkin et al., 2007; O'Connor and Dworkin, 2009; van Hecke et al., 2014), and afflicts over 100 million people, costing up to $650 billion a year in medical treatment and lost productivity in the United States alone (Institute of Medicine (US) Committee on Advancing Pain Research, 2011). Chronic pain is the most common complaint of patients in outpatient clinics (Upshur et al., 2006) and effective therapies remain limited (Meyer-Rosberg et al., 2001; Dworkin et al., 2013).

Attempts to treat pain have often ignore the role of cognitive, attentional, and emotional aspects of pain perception (Bushnell et al., 2013). While animal models have provided indirect evidence, studies in human participants directly demonstrate the ability of emotional and attentional factors to modify pain perception (deCharms et al., 2005; Loggia et al., 2008; Roy et al., 2008, 2011). There is growing evidence that therapies targeting the motivational-cognitive dimensions of pain may be more promising (Auvray et al., 2010).

A key structure for encoding the affective components of multiple modalities is the parabrachial complex (PB). PB regulates satiety and appetite, sleep and arousal, cardiovascular function, and fluid homeostasis (Hajnal et al., 2009; Martelli et al., 2013; Davern, 2014). PB neurons also encode and coordinate behavioral responses to a range of aversive signals, including itch, cachexia, hypercapnia, and visceral malaise, (Campos et al., 2018; Palmiter, 2018; Chiang et al., 2019) and plays a central role in processing acute and chronic pain, (Gauriau and Bernard, 2002; Roeder et al., 2016, 2016; Uddin et al., 2018; Chiang et al., 2019; Raver et al., 2020). Indeed, in multiple models of chronic pain, PB neurons are hyper-responsive and generate amplified neuronal discharges (Matsumoto et al., 1996; Uddin et al., 2018). These amplified discharges are causally related to the expression of pain behaviors (Laird and Bennett, 1993; Asada et al., 1996; Okubo et al., 2013; Raver et al., 2020, 2020).

A potential modulator of PB excitability is the catecholaminergic neurotransmitter norepinephrine (NE). Adrenergic receptors are expressed in PB, and manipulation of NE signaling in PB impacts several behaviors, including food intake (Roman et al., 2016; Boccia et al., 2020; Yang et al., 2021), sodium balance (Andrade et al., 2004) and nociception (Wei and Pertovaara, 2006). NE input to PB arises from multiple cell groups, including the locus coeruleus (A6), but the single largest source is the A2 cell group in the caudal nucleus of the solitary tract (cNTS) (Milner et al., 1986). Neurons in the cNTS are responsive to stress (Rinaman, 2011) and receive exteroceptive input from medullary and spinal dorsal horn neurons (Menetrey and Basbaum, 1987), and interoceptive inputs from the vagus and glossopharyngeal nerves and blood borne signaling molecules (Holt, 2022). Thus, the aversiveness of noxious stimuli may be regulated by the convergence of multimodal inputs within cNTS and its dense noradrenergic projections to PB. However, whether A2 neurons contribute to NE release in PB and its effects on sensory processing within PB are unknown.

We tested the hypothesis that noxious stimuli drive NE release in PB by activating catecholaminergic neurons in cNTS ($cNTS_{cat}$), and that this NE release excites PB neurons and potentiates sensory input to PB. Using a combination of *in vivo* fiber photometry and *in vitro* optogenetics, we find that the A2 to PB circuit can potently facilitate nociceptive signaling in PB.

Materials and Methods

We adhered to accepted standards for rigorous study design and reporting to maximize the reproducibility and translational potential of our findings as described by Landis et al. (2012) and in ARRIVE (Animal Research: Reporting In Vivo Experiments). We performed an *a priori* power analysis to estimate required sample sizes (Landis et al., 2012). All procedures adhered to Animal Welfare Act regulations, Public Health Service guidelines, and approved by the University of Maryland School of Medicine Animal Care and Use Committee.

Animals

We use adult male and female transgenic mice in which Cre recombinase expression is controlled by the tyrosine hydroxylase promotor (TH-Cre) promotor (Savitt et al., 2005). Experimental mice were bred in-house from breeding pairs purchased from the Jackson Laboratory (JAX stock #008601: B6.Cg-7630403G23RikTg(Th-cre)1Tmd/J). We used: 5 male and 3 female mice for *in vivo* fiber photometry recordings from the parabrachial nucleus (PB), 1 male and 2 female mice for *in vivo* stimulation of the caudal nucleus of the solitary tract (cNTS), and 1 male and 4 female mice for *in vitro* recordings. All procedures adhered to Animal Welfare Act regulations, Public Health Service guidelines, and approved by the University of Maryland School of Medicine Animal Care and Use Committee.

Viral construct injection

All viral vector injections were performed in a stereotaxic device under isoflurane anesthesia with Rimadyl for postoperative analgesia. We targeted PB via a small (~1 to 2 mm) craniotomy at 5.2 mm rostral to bregma, 1.5 mm lateral from the midline and injected 500 nL of AAV9-hSyn-NE2h (WZ Biosciences) at a depth of 2.9 mm. We targeted the A2 region of the cNTS by making a small incision in the meninges over the foramen magnum and injected 500 nL of pAAV5-Syn-FLEX-rc[ChrimsonR-tdTomato] (addgene # 62723) at a depth of 0.5 mm, 0.2 mm lateral to the midline at the caudal aspect of the obex. A similar approach was used to target SpVc where we injected 500 nL of pAAV5-Syn-Chronos-GFP (addgene # 59170) at a depth of 0.5 mm, 1.8 mm lateral to the midline. Viral constructs were injected at a rate of 50 nL/min. We waited 3 to 6 weeks for expression prior to recordings.

Fiber Photometry

Mice were anesthetized with an intraperitoneal injection of 2mg/kg urethane, placed on a stereotaxic frame and a fiber optic probe (400 µM diameter, 0.39NA; RWD Life Sciences) was placed in the right PB (-5.2mm AP, +1.5mm ML, -2.2 to -2.5mm DV). The fiber optic probe was connected to a RZX10 LUX fiber photometry processor running Synapse software (Tucker-Davis Technologies) through a Doric mini cube (Doric Lenses). LEDs at 465 nm (30 µW) and 405 nm (10 µW) were used for NE2h excitation and isobestic control respectively. LED power was verified and calibrated as needed using a digital optical power meter (Thor Labs).

Mechanical, thermal and electrical stimulation

We used calibrated forceps to apply a total of 10 consecutive noxious pinch stimuli the right (ipsilateral) and left (contralateral) hindpaw. Resulting changes in NE2h fluorescence were recorded for at least 60 s and consecutive stimuli were spaced 2 minutes apart. We turned the LEDs off between each stimulation to minimize photobleaching of the NE2h sensor.

To generate noxious thermal stimuli, we applied a 5 second heat stimulus to the dorsocaudal edge of the vibrissae pad using a laser (AMD Picasso) with the probe (400 µm) positioned 5 mm from the skin.

The laser was adjusted with a Jenco Electronics microcomputer thermometer to generate 51°C at the end of a 5 s exposure. We waited ≤ 180 s between consecutive stimuli and inspected the skin after each stimulus for tissue damage, which did not occur.

To electrically stimulate $cNTS_{cat}$, we exposed cNTS and inserted a bipolar stimulating electrode (FHC Inc) to a depth of 0.5 mm and applied trains of electrical stimuli at 5, 10, or 20 Hz (0.2 to 2.5s; 80 to 130 µA). We waited a minimum of 2 minutes between trials. Stimuli were applied bilaterally and, since we did not observe a significant difference between stimulation side, the resulting NE2h response metrics were combined for analysis.

Brain slice preparation

We anesthetized animals with ketamine/xylazine, removed their brains, and prepared horizontal or coronal slices (300-µm-thick) containing PB, following the method described by (Ting et al., 2014). For recordings, we placed slices in a submersion chamber and continually perfused (2 ml/min) with ACSF containing (in mM): 119 NaCl, 2.5 KCl, 1.2 NaH2PO4, 2.4 NaHCO3, 12.5 glucose, 2 MgSO4·7H2O, and 2 CaCl2·2H2O.

We obtained whole-cell patch-clamp recordings, in voltage-clamp mode, through pipettes containing (in mM): 120 potassium gluconate, 10 potassium chloride, 10 HEPES, 1 magnesium chloride, 2.5 ATP-Mg, 0.5 EGTA, and 0.2 GTP-Tris. Impedance of patch electrodes was 4 – 8 MΩ. Series resistance (<40 MΩ was monitored throughout the recording, and recordings were discarded if series resistance changed by >20%. All recordings were obtained at room temperature.

To optically activate Chronos or ChrimsonR, we collimated light through a band pass filter and water-immersion 40X microscope objective to achieve whole-field illumination. Light source for each opsin was a single wavelength (470 nm or 550 nm) LED system (CoolLED pE-100, Scientifica, Clarksburg, NJ), controlled through a TTL signal.

Data Analysis

In vivo photometry

We used pMat, developed by the Barker lab (Bruno et al., 2021), to quantify photometry data. Changes in sensor fluorescence were converted to Z-scores using the 5 second window prior to each stimulation (mechanical or thermal) as baseline. Peak Z-score and area under the curve (0 to 60 s post-stimulus) were calculated from the average of all responses. The decay in fluorescence from the initial peak had an initial fast component followed by a slower decay back to baseline. The time constants for these decay rates were calculated by fitting single exponential decay functions to each component.

In vitro recordings

Changes in spontaneous synaptic activity produced by optical stimulation were calculated by measuring the frequency and amplitude of synaptic events 5 to 10 s prior to stimulation and 15 s immediately following the end of the stimulus train. Changes in optically evoked EPSCs from SpVc afferents were measured by averaging the amplitudes of 10 to 15 responses to single or paired pulse optical stimuli, at 10 to 20 s intervals, before and after A2 stimulation. We used a 250 ms, -5 mV square pulse at the end of each stimulation sweep to monitor access resistance and estimate membrane resistance (Rm). The

amplitudes of evoked responses were normalized to changes in Rm by multiplying the average evoked response by the Rm before and after A2 stimulation. Paired pulse ratios (PPR) were calculated by dividing the average amplitude of the EPSC evoked by the second pulse by average of the EPSC amplitude evoked by the first pulse.

Statistics

All statistical comparisons were performed using GraphPad Prism software. When data passed normality tests (D'Agostino & Pearson, Anderson-Darling, and Shapiro-Wilk), we used a paired t-test for comparing before and after or within-animal measures. For data that failed the normality test, we used a paired Wilcoxon test. All mice/cells were included in the analysis, with the exception of the paired pulse ratio data. In this comparison, we only included cells in which the amplitude of the optically evoked EPSC was significantly changed by A2 stimulation as determined by a t-test. As described in the Results, this led to the exclusion of 1 of 6 neurons from PPR analysis. In all tests, a p – value less than 0.05 was considered significant. Data in all graphs are shown as mean/median with 95% confidence intervals unless explicitly stated otherwise in the figure legends.

Results

Noxious stimuli drive prolonged elevations of norepinephrine in PB

The dense innervation of the parabrachial nucleus by noradrenergic afferents suggests that these inputs affect signaling in parabrachial neurons. To test this hypothesis, we studied the prediction that noxious inputs evoke NE release in PB. We used an AAV construct to drive expression of a fluorescent NE sensor (Ne2h) in PB and used fiber photometry to record responses to noxious mechanical and thermal stimuli in anesthetized mice (n = 3 female and 4 male). Changes in fluorescence evoked by these stimuli were normalized to the pre-stimulus levels (ΔF/F) and converted to Z scores for analysis (see Methods). Fluorescence changes were absent in control recordings from 3 mice in which only the reporter (GFP) was expressed in PB.

Figure 1 depicts examples of averaged NE2h signals recorded from PB of the same animal, in response to noxious mechanical stimuli applied to the paw (calibrated pinch; Fig 1A; average of 10 pinches) or thermal stimuli applied to the face (calibrated laser beam; Fig. 1C; average of 5 stimuli). As shown in Figures 1B, C, both stimuli produced a large and long-duration increase in NE2h fluorescence. That the responses were reproducible is evident in the low variance of these responses (Figs. 1A-C).

Response to mechanical stimuli

Noxious mechanical pinch applied to either paw produced, in PB, long-duration increases in NE2h signals. No responses were recorded to light touch or to brush strokes. We quantified the duration of these responses by fitting their decay with a double exponential decay function. Consistent with bilateral projections of the spinoparabrachial pathway (Ding et al., 1995a, 1995b), stimulation applied to either the ipsilateral or the contralateral hindpaw evoked responses of similar duration, and these far outlasted the stimulus. The initial rate of decay had a mean time constant of 5 s for both ipsilateral (95% CI: 2 to 8 s) and contralateral (95% CI: 2 to 7 s) stimuli. The subsequent, slower decay occurred with a mean time constant of 34 s for both ipsilateral (95% CI: 23 to 45 s) and contralateral (95% CI: 16 to 53 s)

stimuli. The latency to the peak response was similar to ipsilateral and contralateral stimuli (mean and 95% CIs: ipsi = 10 s, 8 to 13 s; contra = 10 s, 7 to 12 s; P = 0.24, paired t-test). Thus, noxious mechanical stimulation produced a prolonged increase in NE2h fluorescence in PB that rose and decayed at the same rate, irrespective of the side of the body being stimulated.

The NE2h responses evoked by ipsilateral stimuli were larger than those evoked by stimulating the contralateral hindpaw. Mean peak fluorescence Z scores for ipsilateral stimuli were 24 (95% CIs: 11 to 37) and were larger than those evoked by stimulating the contralateral hind paw (mean Z score with 95% CIs: 19, 11 to 26; P = 0.04, paired t-test). Similarly, the area under the curve (AUC; see Methods) was larger for ipsilateral versus contralateral mechanical stimuli (mean and 95% CIs: ipsi = 970, 400 to 1550; contra = 740, 360 to 1100; P = 0.04, paired t-test).

Response to thermal stimuli

We used a laser to apply noxious heat stimuli (maximum of 51°C, see Methods) to the dorsal aspect of left and right vibrissae pads. Because of the gradual increase in temperature, stimulus onset to thermal stimuli was delayed, compared to responses to the mechanical stimuli (c.f. Fig 1 A & B). NE2h fluorescence peaked 14 s after stimulus onset (95% CIs: ipsi 11 to 16; contra 12 to 15) with a mean peak Z score of 22 (95% CI: 11 to 33) for ipsilateral and 17 (95% CI: 10 to 25) for contralateral stimuli. Neither the peak latency nor the duration of ipsilateral vs contralateral responses was statistically different (P = 0.4, paired t test). The sustained response, measured as AUC over the first 60 s pos-stimulus, was also not different for ipsilateral (mean: 815, 330 to 1300 95% CIs) and contralateral (mean: 812, 400 to 1220 95% CIs) stimuli. As observed with mechanical stimuli, peak NE2h fluorescence decayed in two phases. The initial, rapid decay had a median time constant of 6 s (95% CI: 4 to 56 s) for ipsilateral stimuli and 5 s (95% CI: 3 to 33 s) for contralateral stimuli. This phase was followed by a slower decay, with median time constants of 19 s (95% CI: 5 to 59 s) for ipsilateral and 17 s (95% CI: 3 to 43 s) for contralateral stimuli. The decay rates between ipsilateral and contralateral stimuli were similar ($p > 0.05$, Wilcoxon matched pairs test). These results indicate that noxious thermal stimuli also drive a prolonged increase in NE levels within PB. However, unlike mechanical stimulation, there was no apparent laterality in this effect.

Stimulation of $cNTS_{cat}$ drives prolonged norepinephrine flux in PB

A2 noradrenergic neurons of the caudal nucleus of the solitary tract ($cNTS_{cat}$) are the single largest input of NE to PB. We tested whether these neurons drive NE transients in PB using electrical stimulation of the cNTS in anesthetized mice. We used fiber photometry, as described above, to monitor changes in NE2h fluorescence evoked by 0.2 to 2.5 second stimulus trains applied to cNTS at 5, 10 and 20 Hz (80 to 130 µA). As shown in the representative NE2h responses in Figure 3A, higher stimulation frequencies, at a fixed intensity, produced larger amplitude transients. This result was consistent across 3 mice (Fig. 3B), suggesting that the magnitude of NE transients in PB are proportional to the activity of catecholaminergic neurons of the cNTS. This physiological finding confirms anatomical data demonstrating that A2 provides a major NE inputs to PB (Milner et al., 1986).

A2 Stimulation modulates spontaneous synaptic activity in PB

The observation that NE2h signals remain elevated in PB long after a noxious stimulus suggests that NE afferents may produce long lasting modulation of synaptic transmission in PB. That direct stimulation of

the cNTS also evokes robust, prolonged NE transients suggests that A2 neurons may be a prominent source of this modulation. We tested this hypothesis by asking whether activation of $cNTS_{cat}$ inputs has long-term effects on synaptic activity in PB neurons recorded in a slice preparation. To do this, we expressed the red-shifted opsin ChrimsonR (AAV5-syn-Flex-rc(chrimsonR-tdTomato)) in $cNTS_{cat}$ neurons in 5 mice (4 female, 1 male), allowing us to stimulate these afferents in parabrachial slices. We used a train of optical stimuli (10 Hz, 10 s) because sustained depolarization of presynaptic terminals is required for NE release (Schmidt et al., 2019). As shown in the representative voltage clamp recording in Figure 4A, activation of $cNTS_{cat}$ afferents with a train of optical stimuli evoked a short latency, long duration excitatory postsynaptic current in PB neurons. Spontaneous synaptic activity also increased during $cNTS_{cat}$ activation and remained elevated after the stimulus ended (Fig. 4B; $p = 0.01$, paired t-test, Cohen's $d = 1.1$, $n = 8$ neurons from 5 mice) with a mean increase of 370% (95% CIs: 150 to 590 %) relative to the pre-stimulus period (Fig 4B). $cNTS_{cat}$ stimulation did not affect the amplitude of synaptic events (Fig. 4C; mean: 110% of pre-stimulus amplitudes, 95% CI: 90 to 140 %, $p = 0.7$ paired t-test), despite causing a small reduction in the membrane resistance (Fig. 4D, $p = 0.03$, paired t-test, Cohen's $d = -0.2$) to an average of 87 % (95% CIs: 79 to 96%) of the starting value. The decrease in membrane resistance may reflect activation of postsynaptic adrenergic receptors or arise from the increase in spontaneous synaptic activity.

In a subset of neurons (5 of 8), the increase in spontaneous synaptic activity remained elevated at least 20 s after the $cNTS_{cat}$ stimulation ended. In these cells, we measured the rate of synaptic events at 5 to 20 second intervals and normalized these values to the median frequency prior to $cNTS_{cat}$ stimulation. Using nonlinear regression, we determined that the decay rate for $cNTS_{cat}$ mediated potentiation to be 100 s (95% CI: 50 to 700 s; Fig. 4E). Thus, activation of these afferents *in vitro* produces a sustained increase in synaptic activity in PB neurons with a time course that mirrors the elevation of NE produced *in vivo* by noxious stimuli.

$cNTS_{cat}$ stimulation modulates trigeminal afferents in PB

The parabrachial nucleus subserves a range of exteroceptive and interoceptive modalities. We tested whether NE inputs from $cNTS_{cat}$ specifically affect sensory inputs to parabrachial from spinal trigeminal nucleus caudalis (SpVc). We did this by driving expression of Chronos-GFP in SpVc afferents and a red-shifted opsin, CrimsonR, in $cNTS_{cat}$ neurons of TH-cre mice. In acute brain slices, single or paired pulse optogenetic activation of SpVc afferents reliably evoked EPSCs in PB neurons (Fig 5A). Activation of $cNTS_{cat}$ afferents with train of optical stimuli enhanced the amplitude of EPSCs evoked by stimulating SpVc inputs in 6 of 9 PB neurons, and reduced ($n = 1$), or had no effect on EPSC amplitude in 3 neurons (data from 4 female, 1 male, Mann-Whitney test, $p < 0.05$). In the neurons with potentiated SpVc inputs, the optically evoked SpVc EPSC averaged 154 % of the initial value (95% CIs: 134 to 175%, $p = 0.001$, one sample t-test, theoretical mean = 100%, Cohen's $d = 2.7$),

In 5 of the neurons with potentiated SpVc responses, we examined whether the effects of $cNTS_{cat}$ activation are mediated by presynaptic mechanisms, using optical paired pulse stimulations of SpVc afferents. Paired pulse ratio (PPR, mean of the second response amplitudes divided by the mean amplitude of the first response) decreased following $cNTS_{cat}$ stimulation (mean PPR with 95% CIs: pre = 1.1, 0.8 to 1.3 vs post = 0.86, 0.7 to 1), consistent with an increase in release probability in these excitatory SpVc afferents (Fig. 5C; $p = 0.02$, paired t-test, Cohen's $d = -1.1$)

Discussion

We show that noxious mechanical and thermal stimuli produce a sustained increase in norepinephrine (NE) in the parabrachial nucleus, and that similar increases occur after direct stimulation of the cNTS, a primary source of NE input to PB via the A2 cell group. *In vitro*, photoactivation of noradrenergic afferents from cNTS drives a prolonged increase in excitatory synaptic activity in parabrachial neurons. Activation of these afferents also potentiates synaptic transmission to parabrachial neurons from trigeminal sensory afferents. This occurred in mice of both sexes. Together, these findings indicate that noradrenergic inputs from cNTS to PB may have long lasting faciliatory effects on nociception.

Prolonged NE response to noxious stimuli

Brief noxious mechanical and thermal stimulation caused a sustained increase in NE levels in the parabrachial nucleus, measured with the fluorescent sensor NE2h. Although A2 neurons primarily project to the ipsilateral parabrachial nucleus (Milner et al., 1986), robust NE release was measured in response to noxious stimuli—thermal or mechanical—applied ipsilateral or contralateral to the recorded side. This functional observation is consistent with anatomical studies demonstrating bilateral projections from dorsal horn neurons to the NTS (Menetrey and Basbaum, 1987; Holt et al., 2019; Holt, 2022), and suggests that the noradrenergic response reflects a general aversiveness of sensory inputs, rather than spatial or modality specific information.

The prolonged signal recorded by the NE sensor is unlikely a reflection of the sensor kinetics. Medium and high affinity forms of this sensor (NE1m and NE1h) have off time constants shorter that 2 s (Feng et al., 2019), as does the second generation NE2h sensor used here (personal communication, Y. Li). This decay rate is substantially faster than our observed off-time constants of 17 s for thermal and 34 s for mechanical stimuli. The different decay rates for thermally and mechanically evoked transients also argues against a significant contribution of sensor kinetics to the prolonged signal. Similarly prolonged NE responses to noxious or stressful stimuli have been recorded with microdialysis. For example, noxious pin prick or cold stimuli produced prolonged elevations (up to 15 minutes) in NE levels the dorsal reticular nucleus of neuropathic rats (Fig.3 from (Martins et al., 2015) while intraplantar formalin injection produced a similarly prolonged elevation (~15 minutes) of NE in the bed nucleus of the stria terminalis (BNST) (Deyama et al., 2008). Intermittent tails shocks cause prolonged elevations of NE in the prefrontal cortex and hippocampus of cold-stressed rats (~ 30 to 60 minutes), (Nisenbaum et al., 1991; Gresch et al., 1994). Aversive stimuli also cause NE-dependent prolonged increases in firing rates of amygdala neurons (> 1 hr, Fig 2) (Giustino et al., 2020). Why these different stimulus modalities produce different transient profiles remains to be determined, however, these data indicate that comparatively brief noxious or stressful stimuli produce sustained NE signaling within the CNS, including in the parabrachial nucleus, as reported here.

Source of NE inputs to parabrachial nucleus

NE innervation of the parabrachial nucleus largely originates from the A2 cell group of the NTS (Milner et al., 1986). Tract tracing and lesion studies indicate that the anatomically adjacent locus coeruleus (A6) provides a comparatively minor input to PB (Milner et al., 1986). For these reasons, we focused on the A2 cell group in this study. That the increases in NE in parabrachial evoked by noxious stimuli originate

from A2 afferents is supported by two additional lines of evidence. First, direct stimulation of A2 resulted in prolonged NE transients, similar to those evoked by noxious stimuli (Fig. 3). Second, optogenetic stimulation of NE inputs from A2 evoked, in PB, NE-dependent synaptic responses (discussed below). Nevertheless, we cannot exclude the possibility that NE inputs from other regions, including the locus coeruleus (Yang et al., 2021), contributed to the sensory-evoked NE transients recorded in parabrachial *in vivo*. Additionally, our viral injections targeting A2 may also have transfected adjacent medullary catecholaminergic cells groups, such as A1 and the adrenergic cell groups C1 and C2 although these projections to PB are comparatively minor compared to those from A2 (Milner et al., 1986).

The A2 noradrenergic cell group is part of the visceral NTS within the dorsal vagal complex (DVC) (Rinaman, 2011). The majority of A2 neurons receive monosynaptic excitatory input from the solitary tract (Appleyard et al., 2007) and respond to a wide range of interoceptive and aversive signals (Rinaman, 2011). Caudal NTS neurons also receive direct projections from medullary and dorsal horn neurons, and this overlap has been postulated to aid integration of somatosensory and interoceptive stimuli (Menetrey and Basbaum, 1987; Holt et al., 2019; Holt, 2022). Projections from the caudal NTS, including A2, preferentially target the lateral regions of the parabrachial nucleus (Herbert et al., 1990), including those that participate in nociception and in encoding aversiveness of noxious or stressful stimuli (Palmiter, 2018; Uddin et al., 2018; Bowen et al., 2020; Raver et al., 2020).

In addition to NE, the majority of A2 neurons co-express glutamate, as evidenced by mRNA expression for the vesicular glutamate transporter, VGLUT2, in 80% of A2 neurons (Stornetta et al., 2002) and by *in vitro* experiments where optical stimulation of A2 afferents evokes glutamatergic currents in parabrachial neurons (Roman et al., 2016). Although A2 afferent activation in this study appears to contain a similar glutamatergic component, additional experiments with specific antagonists are needed to determine the relative contributions of glutamatergic and adrenergic receptors to the PB neuron response profiles.

NE increases excitability of parabrachial neurons

To facilitate NE release from $cNTS_{cat}$ afferents, we used brief trains of stimuli known to drive NE release (Schmidt et al., 2019), and that resemble the firing profiles of A2 neurons *in vivo* (Moore and Guyenet, 1985). In neurons, in which the frequency of spontaneous synaptic activity remained elevated for at least 20 s after the stimulus train this facilitation decreased with a time constant of 100 s (Fig 3E). This prolonged effect of $cNTS_{cat}$ activation on synaptic activity *in vitro* is similar to the prolonged NE transients we observe in PB *in vivo* after noxious stimulation (Figs 1 & 2). Similar experiments targeting BNST demonstrate that $cNTS_{cat}$ afferent activation can reliably produce prolonged NE transients *in vitro*. (Schmidt et al., 2019). However, whether the facilitation of synaptic activity following $cNTS_{cat}$ activation observed in our study result from a sustained NE transient remain to be determined.

Our data suggest that the prolonged effects of $cNTS_{cat}$ stimulation on synaptic activity in PB primarily reflect presynaptic mechanisms. Paired pulse ratios (PPR) of optically evoked EPSCs from SpVc terminals were reduced by $cNTS_{cat}$ afferent stimulation, a change thought to reflect an increase in the probability of transmitter release at presynaptic terminals. In addition, the amplitude of the evoked SpVc afferent

responses increased following $cNTS_{cat}$ stimulation, despite a small reduction in membrane resistance. The shift in membrane resistance of PB neurons may reflect a postsynaptic effect of NE or may be a result of the increase in spontaneous synaptic activity produced by $cNTS_{cat}$ stimulation.

Conclusion

We show that NE released from $cNTS_{cat}$ afferents increases excitatory network activity in PB and potentiate sensory inputs to this hub of nociception and aversion. As cNTS is a stress responsive hub for diverse interoceptive and exteroceptive inputs, this connection provides a pathway through which noxious events throughout the body may converge to increase the aversiveness of ongoing or new sources of pain. Understanding the mechanisms through which this occurs may help guide new therapies for treating chronic pain conditions.

References

Andrade CA, Barbosa SP, De Luca LA, Menani JV (2004) Activation of alpha2-adrenergic receptors into the lateral parabrachial nucleus enhances NaCl intake in rats. Neuroscience, 129:25–34.

Appleyard SM, Marks D, Kobayashi K, Okano H, Low MJ, Andresen MC (2007) Visceral afferents directly activate catecholamine neurons in the solitary tract nucleus. J Neurosci, 27:13292–13302.

Asada H, Yamaguchi Y, Tsunoda S, Fukuda Y (1996) Relation of abnormal burst activity of spinal neurons to the recurrence of autotomy in rats. Neurosci Lett, 213:99–102.

Auvray M, Myin E, Spence C (2010) The sensory-discriminative and affective-motivational aspects of pain. Neurosci Biobehav Rev, 34:214–223.

Boccia L, Le Foll C, Lutz TA (2020) Noradrenaline signaling in the LPBN mediates amylin's and salmon calcitonin's hypophagic effect in male rats. FASEB J, 34:15448–15461.

Bowen AJ, Chen JY, Huang YW, Baertsch NA, Park S, Palmiter RD (2020) Dissociable control of unconditioned responses and associative fear learning by parabrachial CGRP neurons. Elife, 9

Bruno CA, O'Brien C, Bryant S, Mejaes JI, Estrin DJ, Pizzano C, Barker DJ (2021) pMAT: An open-source software suite for the analysis of fiber photometry data. Pharmacol Biochem Behav, 201:173093.

Bushnell MC, Ceko M, Low LA (2013) Cognitive and emotional control of pain and its disruption in chronic pain. Nat Rev Neurosci, 14:502–511.

Campos CA, Bowen AJ, Roman CW, Palmiter RD (2018) Encoding of danger by parabrachial CGRP neurons. Nature, 555:617–622.

Chiang MC, Bowen A, Schier LA, Tupone D, Uddin O, Heinricher MM (2019) Parabrachial Complex: A Hub for Pain and Aversion. J Neurosci, 39:8225–8230.

Davern PJ (2014) A role for the lateral parabrachial nucleus in cardiovascular function and fluid homeostasis. Front Physiol, 5:436.

deCharms RC, Maeda F, Glover GH, Ludlow D, Pauly JM, Soneji D, Gabrieli JD, Mackey SC (2005) Control over brain activation and pain learned by using real-time functional MRI. Proc Natl Acad Sci U S A, 102:18626–18631.

Deyama S, Katayama T, Ohno A, Nakagawa T, Kaneko S, Yamaguchi T, Yoshioka M, Minami M (2008) Activation of the beta-adrenoceptor-protein kinase A signaling pathway within the ventral bed nucleus of the stria terminalis mediates the negative affective component of pain in rats. J Neurosci, 28:7728–7736.

Ding YQ, Takada M, Shigemoto R, Mizumo N (1995a) Spinoparabrachial tract neurons showing substance P receptor-like immunoreactivity in the lumbar spinal cord of the rat. Brain Res, 674:336–340.

Ding YQ, Takada M, Shigemoto R, Mizuno N (1995b) Trigeminoparabrachial projection neurons showing substance P receptor-like immunoreactivity in the rat. Neuroscience research,

Dworkin RH, O'Connor AB, Kent J, Mackey SC, Raja SN, Stacey BR, Levy RM, Backonja M, Baron R, Harke H, Loeser JD, Treede RD, Turk DC, Wells CD (2013) Interventional management of neuropathic pain: NeuPSIG recommendations. Pain, 154:2249–2261.

Dworkin RH, White R, O'Connor AB, Baser O, Hawkins K (2007) Healthcare costs of acute and chronic pain associated with a diagnosis of herpes zoster. J Am Geriatr Soc, 55:1168–1175.

Feng J, Zhang C, Lischinsky JE, Jing M, Zhou J, Wang H, Zhang Y, Dong A, Wu Z, Wu H, Chen W, Zhang P, Zou J, Hires SA, Zhu JJ, Cui G, Lin D, Du J, Li Y (2019) A Genetically Encoded Fluorescent Sensor for Rapid and Specific In Vivo Detection of Norepinephrine. Neuron, 102:745–761.e8.

Gauriau C, Bernard JF (2002) Pain pathways and parabrachial circuits in the rat. Exp Physiol, 87:251–258.

Giustino TF, Ramanathan KR, Totty MS, Miles OW, Maren S (2020) Locus Coeruleus Norepinephrine Drives Stress-Induced Increases in Basolateral Amygdala Firing and Impairs Extinction Learning. J Neurosci, 40:907–916.

Gresch PJ, Sved AF, Zigmond MJ, Finlay JM (1994) Stress-induced sensitization of dopamine and norepinephrine efflux in medial prefrontal cortex of the rat. J Neurochem, 63:575–583.

Hajnal A, Norgren R, Kovacs P (2009) Parabrachial coding of sapid sucrose: relevance to reward and obesity. Ann N Y Acad Sci, 1170:347–364.

Herbert H, Moga MM, Saper CB (1990) Connections of the parabrachial nucleus with the nucleus of the solitary tract and the medullary reticular formation in the rat. Journal of Comparative Neurology, 293:540–580.

Holt MK (2022) The ins and outs of the caudal nucleus of the solitary tract: An overview of cellular populations and anatomical connections. J Neuroendocrinol, 34:e13132.

Holt MK, Pomeranz LE, Beier KT, Reimann F, Gribble FM, Rinaman L (2019) Synaptic Inputs to the Mouse Dorsal Vagal Complex and Its Resident Preproglucagon Neurons. J Neurosci, 39:9767–9781.

Institute of Medicine (US) Committee on Advancing Pain Research C, and Education (2011) Relieving Pain in America: A Blueprint for Transforming Prevention, Care, Education, and Research.

Laird JM, Bennett GJ (1993) An electrophysiological study of dorsal horn neurons in the spinal cord of rats with an experimental peripheral neuropathy. J Neurophysiol, 69:2072–2085.

Landis SC, Amara SG, Asadullah K, Austin CP, Blumenstein R, Bradley EW, Crystal RG, Darnell RB, Ferrante RJ, Fillit H, Finkelstein R, Fisher M, Gendelman HE, Golub RM, Goudreau JL, Gross RA, Gubitz AK, Hesterlee SE, Howells DW, Huguenard J, Kelner K et al. (2012) A call for transparent reporting to optimize the predictive value of preclinical research. Nature, 490:187–191.

Loggia ML, Mogil JS, Bushnell MC (2008) Experimentally induced mood changes preferentially affect pain unpleasantness. J Pain, 9:784–791.

Martelli D, Stanić D, Dutschmann M (2013) The emerging role of the parabrachial complex in the generation of wakefulness drive and its implication for respiratory control. Respir Physiol Neurobiol, 188:318–323.

Martins I, Carvalho P, de Vries MG, Teixeira-Pinto A, Wilson SP, Westerink BHC, Tavares I (2015) Increased noradrenergic neurotransmission to a pain facilitatory area of the brain is implicated in facilitation of chronic pain. Anesthesiology, 123:642–653.

Matsumoto N, Bester H, Menendez L, Besson JM, Bernard JF (1996) Changes in the responsiveness of parabrachial neurons in the arthritic rat: an electrophysiological study. J Neurophysiol, 76:4113–4126.

Menetrey D, Basbaum AI (1987) Spinal and trigeminal projections to the nucleus of the solitary tract: a possible substrate for somatovisceral and viscerovisceral reflex activation. Journal of Comparative Neurology, 255:439–450.

Meyer-Rosberg K, Kvarnström A, Kinnman E, Gordh T, Nordfors LO, Kristofferson A (2001) Peripheral neuropathic pain--a multidimensional burden for patients. Eur J Pain, 5:379–389.

Milner TA, Joh TH, Pickel VM (1986) Tyrosine hydroxylase in the rat parabrachial region: ultrastructural localization and extrinsic sources of immunoreactivity. J Neurosci, 6:2585–2603.

Moore SD, Guyenet PG (1985) Effect of blood pressure on A2 noradrenergic neurons. Brain research, 338:169–172.

Nisenbaum LK, Zigmond MJ, Sved AF, Abercrombie ED (1991) Prior exposure to chronic stress results in enhanced synthesis and release of hippocampal norepinephrine in response to a novel stressor. J Neurosci, 11:1478–1484.

O'Connor AB, Dworkin RH (2009) Treatment of neuropathic pain: an overview of recent guidelines. Am J Med, 122:S22–32.

Okubo M, Castro A, Guo W, Zou S, Ren K, Wei F, Keller A, Dubner R (2013) Transition to persistent orofacial pain after nerve injury involves supraspinal serotonin mechanisms. J Neurosci, 33:5152–5161.

Palmiter RD (2018) The Parabrachial Nucleus: CGRP Neurons Function as a General Alarm. Trends Neurosci, 41:280–293.

Raver C, Uddin O, Ji Y, Li Y, Cramer N, Jenne C, Morales M, Masri R, Keller A (2020) An Amygdalo-Parabrachial Pathway Regulates Pain Perception and Chronic Pain. J Neurosci, 40:3424–3442.

Rinaman L (2011) Hindbrain noradrenergic A2 neurons: diverse roles in autonomic, endocrine, cognitive, and behavioral functions. Am J Physiol Regul Integr Comp Physiol, 300:R222–35.

Roeder Z, Chen Q, Davis S, Carlson JD, Tupone D, Heinricher MM (2016) Parabrachial complex links pain transmission to descending pain modulation. Pain, 157:2697–2708.

Roman CW, Derkach VA, Palmiter RD (2016) Genetically and functionally defined NTS to PBN brain circuits mediating anorexia. Nat Commun, 7:11905.

Roy M, Lebuis A, Peretz I, Rainville P (2011) The modulation of pain by attention and emotion: a dissociation of perceptual and spinal nociceptive processes. Eur J Pain, 15:641.e1–10.

Roy M, Peretz I, Rainville P (2008) Emotional valence contributes to music-induced analgesia. Pain, 134:140–147.

Savitt JM, Jang SS, Mu W, Dawson VL, Dawson TM (2005) Bcl-x is required for proper development of the mouse substantia nigra. J Neurosci, 25:6721–6728.

Schmidt KT, Makhijani VH, Boyt KM, Cogan ES, Pati D, Pina MM, Bravo IM, Locke JL, Jones SR, Besheer J, McElligott ZA (2019) Stress-Induced Alterations of Norepinephrine Release in the Bed Nucleus of the Stria Terminalis of Mice. ACS Chem Neurosci, 10:1908–1914.

Stornetta RL, Sevigny CP, Guyenet PG (2002) Vesicular glutamate transporter DNPI/VGLUT2 mRNA is present in C1 and several other groups of brainstem catecholaminergic neurons. J Comp Neurol, 444:191–206.

Ting JT, Daigle TL, Chen Q, Feng G (2014) Acute Brain Slice Methods for Adult and Aging Animals: Application of Targeted Patch Clamp Analysis and Optogenetics. In: Methods in Molecular Biology: Patch-Clamp Methods and Protocols eds), pp 221–242. New York, NY: Springer New York.

Uddin O, Studlack P, Akintola T, Raver C, Castro A, Masri R, Keller A (2018) Amplified parabrachial nucleus activity in a rat model of trigeminal neuropathic pain. Neurobiol Pain, 3:22–30.

Upshur CC, Luckmann RS, Savageau JA (2006) Primary care provider concerns about management of chronic pain in community clinic populations. J Gen Intern Med, 21:652–655.

van Hecke O, Austin SK, Khan RA, Smith BH, Torrance N (2014) Neuropathic pain in the general population: a systematic review of epidemiological studies. Pain, 155:654–662.

Wei H, Pertovaara A (2006) Spinal and pontine alpha2-adrenoceptors have opposite effects on pain-related behavior in the neuropathic rat. Eur J Pharmacol, 551:41–49.

Yang B, Sanches-Padilla J, Kondapalli J, Morison SL, Delpire E, Awatramani R, Surmeier DJ (2021) Locus coeruleus anchors a trisynaptic circuit controlling fear-induced suppression of feeding. Neuron, 109:823–838.e6.

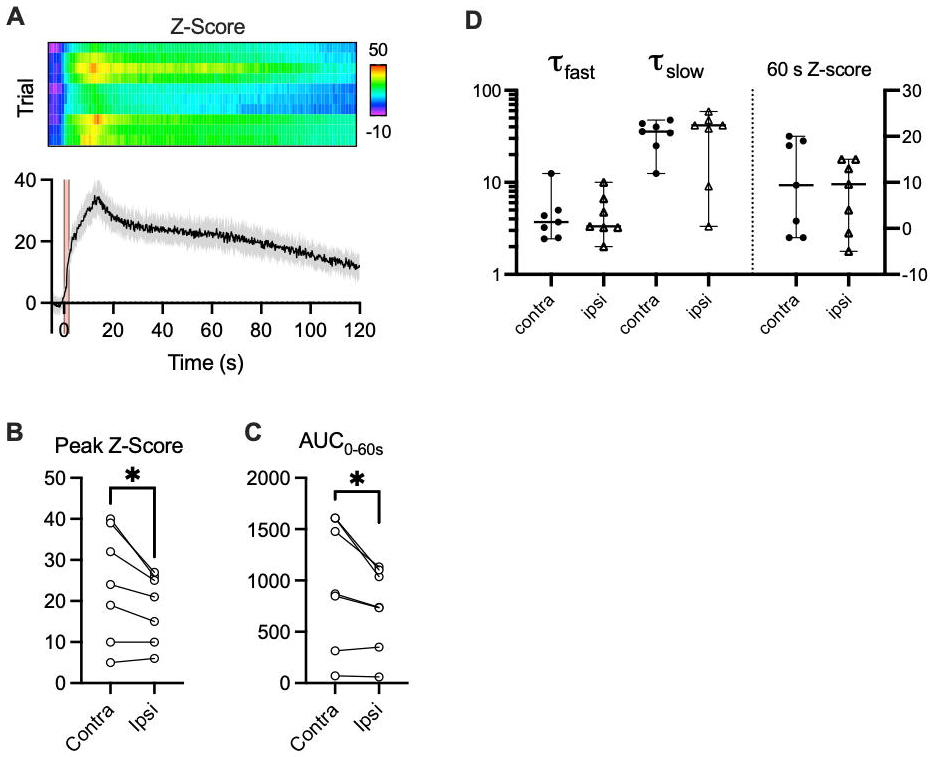

Figure 1: Noxious mechanical stimuli generate prolonged NE transients in PB. **(A)** Heat map of NE2h fluorescence (bottom, Z-score normalized) evoked by noxious pinch of the hindpaw in an anesthetized mouse. The average response to 10 trials (with 95% CIs) shows the prolonged duration of the sensor responses to the brief stimuli. Peak response magnitude **(B)** and area under the curve (AUC)**(C)** for 7 mice in which the left and right hindpaw was stimulated while monitoring fluorescence in the right PB. (D) After the peak, the rate of decay in fluorescent intensity had two components and time constants (τ_{fast} and τ_{slow}) were obtained by fitting these components with an exponential decay function. In addition to the slow rate of decay, the fluorescence remained elevated for more than 60 seconds in 5 of 7 mice.

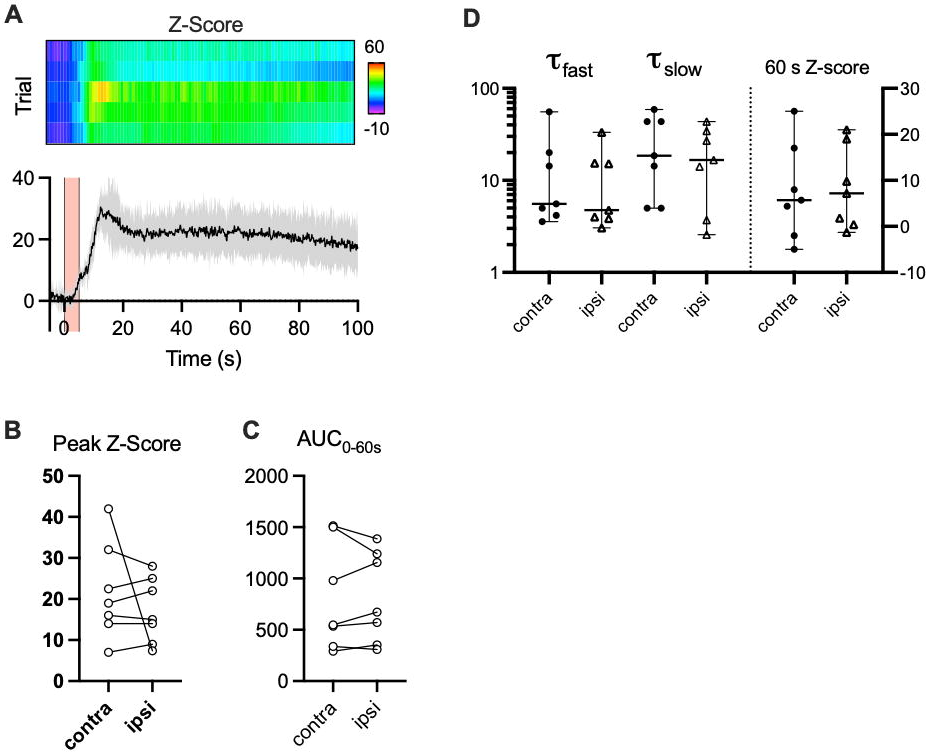

Figure 2: Noxious thermal stimuli generate prolonged NE transients in PB. **(A)** Heat map of NE2h fluorescence (bottom, Z-score normalized) evoked by noxious heat applied caudal to the vibrissae pad in an anesthetized mouse. The average response to 5 trials (with 95% CIs) shows the prolonged duration of the sensor responses to the brief stimuli. Peak response magnitude **(B)** and area under the curve (AUC)**(C)** for 7 mice in which the left and right face was stimulated while monitoring fluorescence in the right PB. **(D)** After the peak, the rate of decay in fluorescent intensity had two components and time constants (τ_{fast} and τ_{slow}) were obtained by fitting these components with an exponential decay function. In addition to the slow rate of decay, the fluorescence remained elevated for more than 60 seconds in 4 of 7 mice.

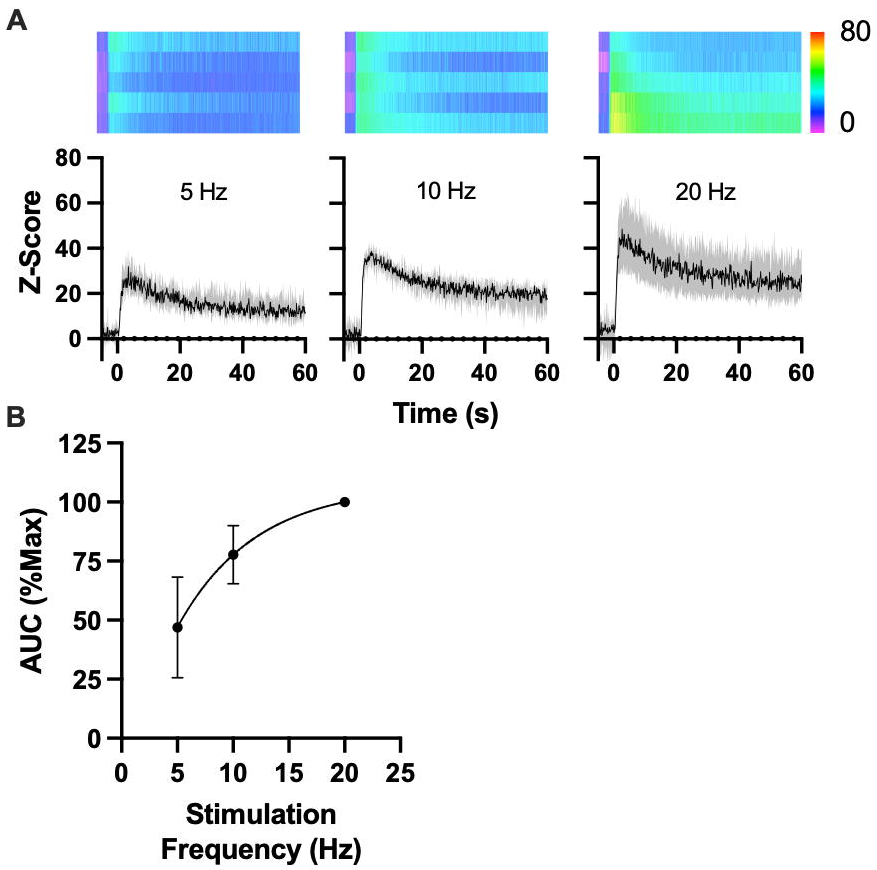

Figure 3: Electrical stimulation of cNTS evokes NE transients in PB. **(A)** Z-score heat maps of individual trials (top row) and averaged responses (bottom row, mean with 95% CIs) of NEsensor fluorescence in PB evoked by electrical stimulation of cNTS at 5, 10 and 20 Hz. **(B)** Group data from 3 mice indicate the magnitude of NE transients are proportional to the frequency of stimulation. Data in (B) are normalized to the response at 20 Hz.

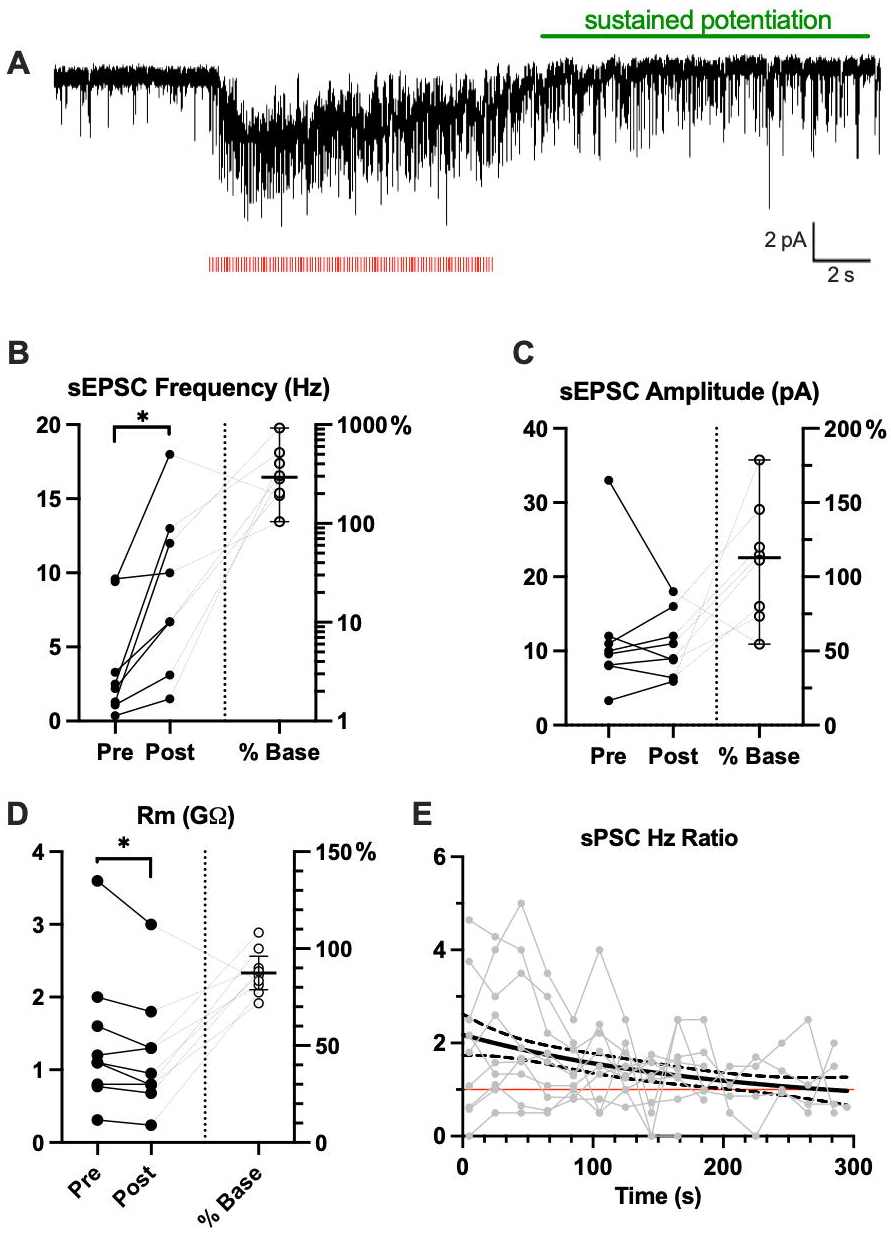

Figure 4: $cNTS_{cat}$ afferent stimulation potentiates excitatory synaptic transmission in PB. **(A)** Representative voltage clamp recording from a PB neuron showing the sustained increase in spontaneous synaptic activity after A2 afferent stimulation (10 Hz, 10 s, red bars). **(B)** Synaptic activity increased to a mean of 370% of pre-stimulation values in 8 neurons. There was no effect of $cNTS_{cat}$ stimulation on event amplitude **(C)**, despite a small reduction in membrane resistance **(D)**. The $cNTS_{cat}$ -evoked increase in sEPSC frequency was prolonged in 5 neurons and decayed back to pre-stimulus values with a time constant of 100 s.

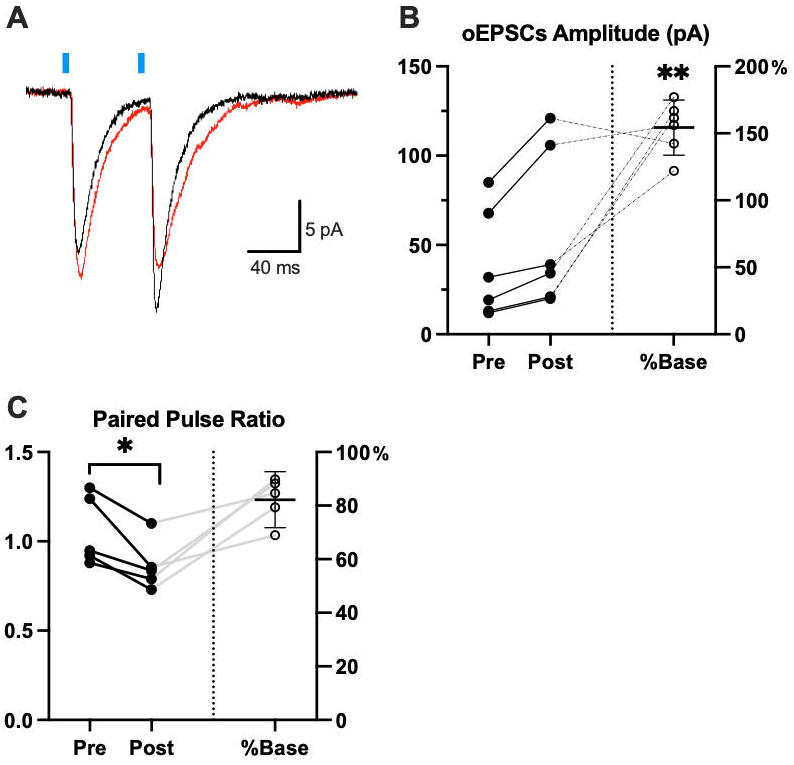

Figure 5: $cNTS_{cat}$ stimulation potentiates sensory inputs to PB neurons. **(A)** Representative EPSCs in PB neurons evoked by paired optical stimulation of SpVc afferent terminals before (black) and after (red) $cNTS_{cat}$ optical afferent stimulation. **(B)** EPSCs evoked were significantly increased by $cNTS_{cat}$ activation in 6 of 9 PB neurons by an average of 154 %. **(C)** Paired pulse ratio (PPR) was reduced to 88% of the baseline value (95% CIs: 72 to 103%) in 5 cells in which $cNTS_{cat}$ stimulation significantly potentiated the amplitude of SpVc EPSCs.